Dynamics of a fluid inside a precessing cylinder

Romain Lagrange, Patrice Meunier, Christophe Eloy, François Nadal

Mécanique & Industries 10, 187–194 (2009)
© AFM, EDP Sciences 2009
DOI: 10.1051/meca/2009048

www.mecanique-industries.org

Mécanique & Industries

Dynamics of a fluid inside a precessing cylinder

Romain Lagrange[1,a], Patrice Meunier[1], Christophe Eloy[1] and François Nadal[2]

[1] Institut de Recherche sur les Phénomènes Hors Équilibre / Université de Provence, IRPHE – UMR 6594, Technopôle de Château-Gombert, 49, rue Joliot Curie, B.P. 146, 13384 Marseille Cedex 13, France
[2] Commissariat à l'Énergie Atomique (CEA/CESTA), France

Received 20 April 2009

Abstract – The instability of a fluid inside a precessing cylinder is studied theoretically and experimentally. This study is motivated by aeronautics and geophysics applications. Precessional motion forces hydrodynamics waves called Kelvin modes whose structure and amplitude are predicted by a linear inviscid theory. When a forced Kelvin mode is resonant, a viscous and weakly nonlinear theory has been developed to predict its saturated amplitude. We show that this amplitude scales as $Re^{1/2}$ for low Reynolds numbers and as $\theta^{1/3}$ (where θ is the precessing angle) for high Reynolds numbers. These scalings are confirmed by PIV measurements. For Reynolds numbers sufficiently large, this forced flow becomes unstable. A linear stability analysis based on a triadic resonance between a forced Kelvin mode and two free modes has been carried out. The precessing angle for which the flow becomes unstable is predicted and compared successfully to experimental measurements. A weakly nonlinear theory was developed and allowed to show that the bifurcation of the instability of precession is subcritical. It also showed that, depending on the Reynolds number, the unstable flow can be steady or intermittent. Finally, this weakly nonlinear theory allowed to predict, with a good agreement with experiments, the mean flow in the cylinder; even if it is turbulent.

Key words: Precession / Kelvin modes / instability / triadic resonance

Résumé – Dynamique d'un fluide dans un cylindre en précession. L'instabilité d'un fluide dans un cylindre en précession est étudiée théoriquement et expérimentalement. Les domaines d'application de cette étude se retrouvent en aéronautique et en géophysique. La précession force des ondes hydrodynamiques appelées modes de Kelvin, dont la structure et l'amplitude sont prédites par une théorie linéaire non visqueuse. Quand un mode de Kelvin forcé est résonnant, une théorie visqueuse et faiblement non linéaire a été développée pour prédire la saturation de son amplitude. Nous montrons que cette amplitude varie comme $Re^{1/2}$ pour des faibles nombres de Reynolds, et comme $\theta^{1/3}$ (θ étant l'angle de précession) pour les grands nombres de Reynolds. Ces scalings sont confirmés par des mesures PIV. Pour des nombres de Reynolds suffisamment grands l'écoulement forcé devient instable. Une analyse de stabilité linéaire basée sur un mécanisme de résonance triadique entre le mode de Kelvin forcé et deux modes de Kelvin libres a été développée. L'angle de précession pour lequel l'écoulement devient instable est prédit et confirmé par les expériences. Une théorie faiblement non linéaire a été développée et a permis de montrer que la bifurcation de l'instabilité est sous critique. Cette théorie a également montré qu'en fonction du nombre de Reynolds, l'écoulement instable peut être stationnaire ou intermittent. Finalement cette théorie faiblement non linéaire permet de prédire, en bon accord avec les expériences, l'écoulement moyen dans le cylindre, même lorsque cet écoulement est turbulent.

Mots clés : Précession / modes de Kelvin / instabilité / résonance triadique

[a] Corresponding author: lagrange@irphe.univ-mrs.fr

Article published by EDP Sciences

Nomenclature

A	Amplitude of the resonant base flow
A^*	Complex conjugate of A
A_0	Amplitude of the geostrophic mode
A_1	Amplitude of the first free Kelvin mode
A_2	Amplitude of the second free Kelvin mode
d_2	Second root of the Bessel function of the first kind and of order 5
f	Forcing parameter
H	Cylinder height
h	Aspect ratio of the cylinder
i	Complex number $\sqrt{-1}$
J_m	Bessel function of the first kind and of order m
$J_m^{'}$	Derivative of J_m
k	Axial wavenumber of the resonant base flow
k_1	Axial wavenumber of the first free Kelvin mode
k_2	Axial wavenumber of the second free Kelvin mode
m	Azimuthal wavenumber of the resonant base flow
m_1	Azimuthal wavenumber of the first free Kelvin mode
m_2	Azimuthal wavenumber of the second free Kelvin mode
N_1	Non-linear coupling term between the resonant base flow and the second free Kelvin mode
N_2	Non-linear coupling term between the resonant base flow and the first free Kelvin mode
R	Radius of the cylinder
r	Classical cylindrical coordinate
Re	Reynolds number
Ro	Rossby number
S_1	Boundary viscous effects for the first free Kelvin mode
S_2	Boundary viscous effects for the second free Kelvin mode
$\mathbf{u}_\varphi$	Classical unit vector of the cylindrical base
V_1	Volume viscous effects for the first free Kelvin mode
V_2	Volume viscous effects for the second free Kelvin mode
z	Cylindrical coordinate along the cylinder axis. $z = 0$ being the mid-height of the cylinder
δ	Parameter of the constitutive relation for the resonant base flow
δ_1	Parameter of the constitutive relation for the first free Kelvin mode
δ_2	Parameter of the constitutive relation for the second free Kelvin mode
σ	Growth rate of the instability
θ	Precessing angle
ν	Kinematic viscosity
ξ	Interaction coefficient between the geostrophic mode and the resonant base flow
ξ_1	Interaction coefficient between the geostrophic mode and the first free Kelvin mode
ξ_2	Interaction coefficient between the geostrophic mode and the second free Kelvin mode
φ	Classical cylindrical coordinate
χ_1	Non-linear coefficient for the first free Kelvin mode
χ_2	Non-linear coefficient for the second free Kelvin mode
Ω	Axial component of the fluid rotation vector
Ω_1	Angular frequency of the cylinder
ω_1	Dimensionless angular frequency of the first free Kelvin mode
Ω_2	Angular frequency of the platform, rad.s^{-1}
ω_2	Dimensionless angular frequency of the second free Kelvin mode
ω	Frequency ratio

1 Introduction

The knowledge of the flow forced by a precessional motion is of critical importance in several domains. In aeronautics, a flying object whose liquid propellant is forced by precession can have its trajectory dangerously modified. In geophysics the Earth precession modifies the flow of its liquid core and is therefore of significative importance in understanding the dynamo effect (among other effects such as convection, boundary layers, elliptic or tidal instability [1]).

Experiments such as the one carried out by McEwan [2] clearly show that the container precession forces a flow which can be decomposed as a sum of inertial waves (also called Kelvin modes). For low Reynolds numbers this flow is stable. For large Reynolds numbers it becomes unstable and can degenerate into a turbulent flow. This behavior was also reported by Manasseh [3–5], and Kobine [6]. Among several scenarios, Kerswell [7] suggested that a given Kelvin mode can trigger a triadic resonance with two other Kelvin modes leading to an instability. We have demonstrated that this mechanism of triadic resonance between Kelvin modes (which bears similarity with the elliptic instability [8,9]) is indeed responsible of the instability of precession.

The paper is organized as follows. Section 2 is dedicated to a presentation of the problem. Parameters and dimensionless numbers are introduced and a short presentation of the experimental set-up is described. In Section 3 the base flow, ie. the flow before the instability, is presented. Classical results concerning a non-resonant flow are recalled and extended in the case of a resonant flow. In Section 4 the instability is experimentally presented and a linear stability analysis is described. Finally, a weakly nonlinear theory is developed in Section 5 in order to explain the transition from an unstable and stationary flow to an unstable and intermittent flow.

2 Presentation of the problem

The flow inside a precessing cylinder of height H and radius R, full of fluid of kinematic viscosity ν is considered. This cylinder rotates at the angular frequency Ω_1 around its axis. It is mounted on a platform which rotates at the angular frequency Ω_2 as shown in Figure 1. The angle between the two axes of rotation is the precession angle θ. In the following, variables are made dimensionless by using R and $\Omega = \Omega_1 + \Omega_2 \cos\theta$ as characteristic length and frequency. The dynamics of this precessing system depends on four dimensionless numbers:

- the aspect ratio $h = H/R$;
- the frequency ratio $\omega = \Omega_1/\Omega$;
- the Rossby number $Ro = \Omega_2 \sin\theta/\Omega$;
- the Reynolds number $Re = \Omega R^2/\nu$.

An experimental set-up was built in the laboratory, allowing Particle Image Velocimetry (PIV) measurements of the velocity fields in a transverse section of the cylinder.

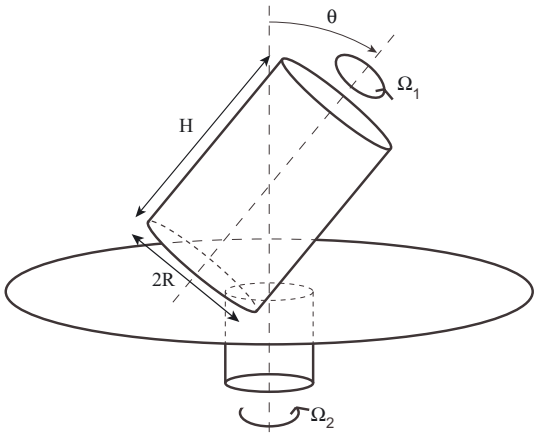

Fig. 1. Sketch of a precessing cylinder.

To perform the acquisition of a PIV field, small markers illuminated with a thin light sheet created by a Yag pulsed laser were used. Particle images were recorded by a camera mounted on the rotating platform. The horizontal velocity and the axial vorticity fields in the cylinder frame of reference were thus measured. More details about PIV treatment can be found in [10] and a precise description of the experimental set-up is given in [11].

3 Base flow

In Figure 2a the axial flow vorticity is showed in the cylinder reference frame for a small Rossby number: $Ro = 0.0031$, and a moderate Reynolds number: $Re = 3500$. Two counter rotating vortices are observed. It corresponds to a Kelvin mode which is forced by precession. Owing to the time and azimuthal dependence of the precession forcing, this Kelvin mode has an azimuthal wavenumber $m = 1$ and an angular frequency ω (see [12]). Its velocity field is

$$\mathbf{V_b} = A\mathbf{v_b}(r,z)\,\mathrm{e}^{\mathrm{i}(\omega t+\varphi)} + \text{c.c} \tag{1}$$

where A is the amplitude, c.c denotes the complex conjugate and

$$\mathbf{v_b}(r,z) = \begin{pmatrix} u_b(r)\sin(kz) \\ v_b(r)\sin(kz) \\ w_b(r)\cos(kz) \end{pmatrix}$$

$$\text{with} \begin{cases} u_b(r) = \mathrm{i}\dfrac{\omega r\delta J_1'(\delta r) + 2J_1(\delta r)}{2r(\omega^2-4)} \\ v_b(r) = \dfrac{2r\delta J_1'(\delta r) + \omega J_1(\delta r)}{2r(4-\omega^2)} \\ w_b(r) = \mathrm{i}\dfrac{k}{2\omega}J_1(\delta r) \end{cases} \tag{2}$$

In this expression $J_1(r)$ is the Bessel function of the first kind and $J_1'(r)$ its r-derivative.

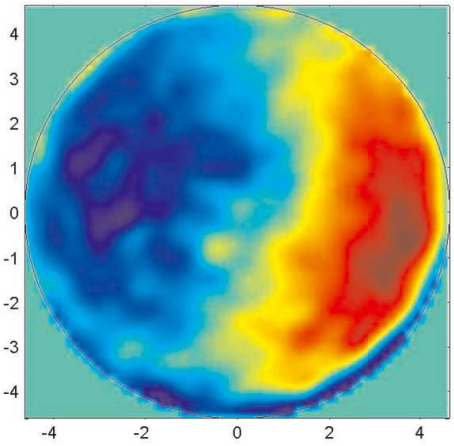

(a)

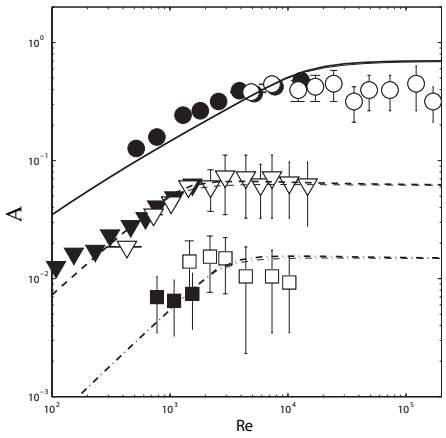

(b)

Fig. 2. (a) Vorticity field of the first Kelvin mode measured by PIV at its first resonance, in the absence of instability ($h = 1.62$, $\omega = 1.18$, $Re \approx 3500$, $Ro = 0.0031$). (b) Amplitude of the first Kelvin mode obtained at the first (solid line), second (dashed line) and third (dotted line) resonance. Symbols are experimental results ($h = 1.8$, $\theta = 2^\circ$).

The parameter δ satisfies the constitutive relation

$$\delta^2 = \frac{4-\omega^2}{\omega^2}k^2 \tag{3}$$

where the axial wavenumber k depends on ω according to the following dispersion relation with $m = 1$

$$\omega\delta J_m^{'}(\delta) + 2mJ_m(\delta) = 0 \tag{4}$$

At a given ω this dispersion relation has an infinite number of solutions. Each solution corresponds to a Kelvin mode forced at the frequency ω. The Kelvin mode showed in Figure 2 is the first Kelvin mode. It corresponds to the mode with the smallest axial wavenumber k.

A classical linear and inviscid theory can predict the amplitude A of a forced Kelvin mode. This theory shows that $A \sim Ro$ and depends on ω. However, when the mode is resonant (i.e. $k = n\pi/h$, with n an odd number) its amplitude A diverges. A viscous [13] and weakly nonlinear [11] theory is then necessary to predict the amplitude saturation. Figure 2b represents the saturation of the first Kelvin mode as a function of Re for its first three resonances. We showed [11] that for small Reynolds numbers (viscous regime, $\mathrm{Re}^{1/2}\mathrm{Ro}^{2/3} \ll 1$), A scales as $Ro\sqrt{Re}$ due to viscous effects in the Ekman layers. For larger Reynolds numbers (nonlinear regime, $\mathrm{Re}^{1/2}\mathrm{Ro}^{2/3} \gg 1$)), A scales as $Ro^{1/3}$. Predictions of [11] are in good agreement with PIV measurements represented by symbols in Figure 2b.

4 Instability

As shown in the literature [5,6], the flow inside a precessing cylinder becomes unstable when the Reynolds or the Rossby number is increased. Figure 3 is a PIV measurement of the axial and instantaneous vorticity field for $\mathrm{Re} = 6500$ and $Ro = 0.0031$. For such a value of Re and Ro the flow depicted in Figure 2a is unstable and the unstable mode exhibits a ring with 10 lobes of vorticity with alternate signs. It corresponds to a free Kelvin mode with azimuthal wavenumber $m_1 = 5$. Its velocity field is

$$\mathbf{V_1} = A_1\mathbf{v_1}(r,z)\,\mathrm{e}^{\mathrm{i}(\omega_1 t + m_1\varphi)} + \mathrm{c.c} \tag{5}$$

where

$$\mathbf{v}_1(r,z) = \begin{pmatrix} u_1(r)\sin(k_1 z) \\ v_1(r)\sin(k_1 z) \\ w_1(r)\cos(k_1 z) \end{pmatrix}$$

$$\text{with} \begin{cases} u_1(r) = 2\mathrm{i}\dfrac{\omega_1 r\delta_1 J_{m_1}^{'}(\delta_1 r) + 2m_1 J_{m_1}(\delta_1 r)}{r(\omega_1^2 - 4)} \\ v_1(r) = 2\dfrac{2r\delta_1 J_{m_1}^{'}(\delta_1 r) + m_1\omega_1 J_{m_1}(\delta_1 r)}{r(4-\omega_1^2)} \\ w_1(r) = 2\mathrm{i}\dfrac{k_1}{\omega_1}J_{m_1}(\delta_1 r) \end{cases} \tag{6}$$

In (5) and (6), ω_1 is the dimensionless frequency of the mode $m_1 = 5$ and k_1 its axial wavenumber. The parameter δ_1 satisfies the constitutive relation (3) with ω_1 and k_1 instead of ω and k. Parameters ω_1 and δ_1 also satisfy the dispersion relation (4) with $m = 5$.

If the position of the PIV laser sheet is moved from $z = h/4$ to $z = 0$ (mid-height of the cylinder) a second free Kelvin mode is observed. It exhibits 12 lobes of vorticity with alternate signs and thus corresponds to a free Kelvin mode whose azimuthal wavenumber is $m_2 = 6$. Its velocity field is

$$\mathbf{V_2} = A_2\mathbf{v_2}(r,z)\,\mathrm{e}^{\mathrm{i}(\omega_2 t + m_2\varphi)} + \mathrm{c.c} \tag{7}$$

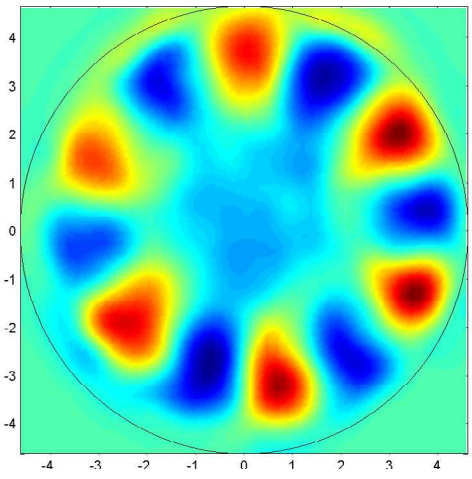

(a)

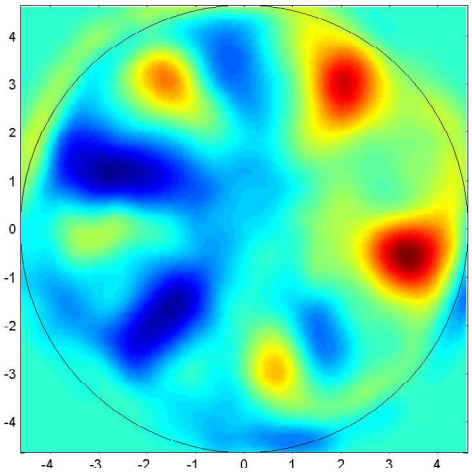

(b)

Fig. 3. Vorticity field of the free modes which constitute the instability of a precessing cylinder. (a) Vorticity field measured at mid-height of the cylinder. (b) Vorticity field measured at $z = h/4$ showing the mode $m = 5$ superimposed with the forced Kelvin mode of Figure 2a ($h = 1.62$, $\omega = 1.18$, $Re \approx 6000$, $Ro = 0.0031$).

where

$$\mathbf{v}_2(r,z) = \begin{pmatrix} u_2(r)\cos(k_2 z) \\ v_2(r)\cos(k_2 z) \\ w_2(r)\sin(k_2 z) \end{pmatrix}$$

$$\text{where} \begin{cases} u_2(r) = 2\dfrac{\omega_2 r\delta_2 J'_{m_2}(\delta_2 r) + 2m_2 J_{m_2}(\delta_2 r)}{r(\omega_2^2 - 4)} \\ v_2(r) = 2\mathrm{i}\dfrac{2r\delta_2 J'_{m_2}(\delta_2 r) + m_2\omega_2 J_{m_2}(\delta_2 r)}{r(\omega_2^2 - 4)} \\ w_2(r) = -2\dfrac{k_2}{\omega_2} J_{m_2}(\delta_2 r) \end{cases} \tag{8}$$

In (7) and (8), ω_2 is the dimensionless frequency of the mode $m_2 = 6$ and k_2 its axial wavenumber. The parameter δ_2 satisfies the constitutive relation (3) with ω_2 and k_2 instead of ω and k. Parameters ω_2 and δ_2 also satisfy the dispersion relation (4) with $m = 6$.

The frequencies of the two free Kevin modes shown in Figure 3 were experimentally measured and their axial wavenumbers were deduced. We have demonstrated that the resonant base flow and the free Kelvin modes satisfy the resonant condition $m_2 - m_1 = 1$, $\omega_2 - \omega_1 = \omega$ and $k_2 - k_1 = k$. This corresponds to a mechanism of triadic resonance between the three Kelvin modes.

More information about experimental results presented here can be found in [14].

To better confirm this mechanism of triadic resonance, a linear stability analysis has been developed. The first step is to find the free Kelvin modes satisfying the resonant condition. They correspond to the crossing points of the two dispersion relations shown in Figure 4a. When these points are determined, the structure of the associated free Kelvin modes is known. Then, because of a solvability condition, equations of evolution for the amplitudes A_1 and A_2 of the two free Kelvin modes can be obtained. If the base flow is a forced Kelvin mode of amplitude A, these equations are

$$\begin{cases} \partial_t A_1 = A^* N_1 A_2 - \frac{1}{\sqrt{Re}} S_1 A_1 - \frac{1}{Re} V_1 A_1 \\ \partial_t A_2 = A N_2 A_1 - \frac{1}{\sqrt{Re}} S_2 A_2 - \frac{1}{Re} V_2 A_2 \end{cases} \tag{9}$$

where

$$N_1 = \mathrm{i}\pi h\left(\frac{k}{\omega} - \frac{k_2}{\omega_2}\right)\int_0^1 \begin{vmatrix} u_2 & u_b^* & u_1^* \\ v_2 & v_b^* & v_1^* \\ w_2 & w_b^* & w_1^* \end{vmatrix} r\mathrm{d}r \Big/ \mathbf{v_1}\odot\mathbf{v_1} \tag{10}$$

$$N_2 = \mathrm{i}\pi h\left(\frac{k}{\omega} - \frac{k_1}{\omega_1}\right)\int_0^1 \begin{vmatrix} u_b & u_1 & u_2^* \\ v_b & v_1 & v_2^* \\ w_b & w_1 & w_2^* \end{vmatrix} r\mathrm{d}r \Big/ \mathbf{v_2}\odot\mathbf{v_2} \tag{11}$$

where $|.|$ is the determinant and the scalar product $\odot$ between two vectors $\mathbf{U_1} = (U_{1r}, U_{1\varphi}, U_{1z})$ and $\mathbf{U_2} = (U_{2r}, U_{2\varphi}, U_{2z})$ being defined as

$$\mathbf{U_1}\odot\mathbf{U_2} = \int_0^1\int_0^{2\pi}\int_{-h/2}^{h/2}\left(U_{1r}^* U_{2r} + U_{1\varphi}^* U_{2\varphi} + U_{1z}^* U_{2z}\right) \times r\,\mathrm{d}r\,\mathrm{d}\varphi\,\mathrm{d}z \tag{12}$$

The terms N_1 and N_2 represent the interaction, through the nonlinear term of the Navier Stokes equation, of a free Kelvin mode with the resonant base mode. The terms $1/Re$ represent the influence of volume viscous effects and terms $1/\sqrt{Re}$ the influence of boundary viscous effects through Ekman suction. Constants S_1, S_2, V_1, V_2 can be

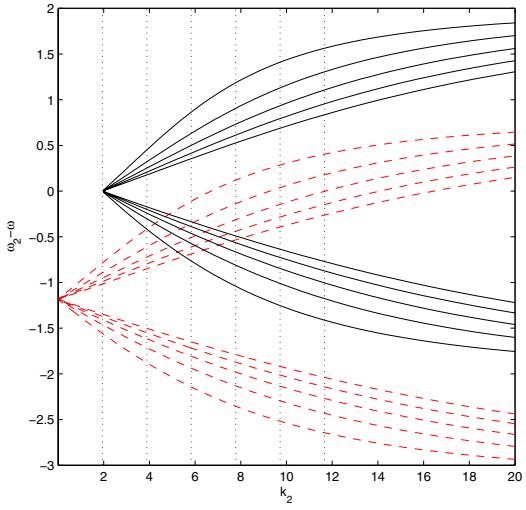

(a)

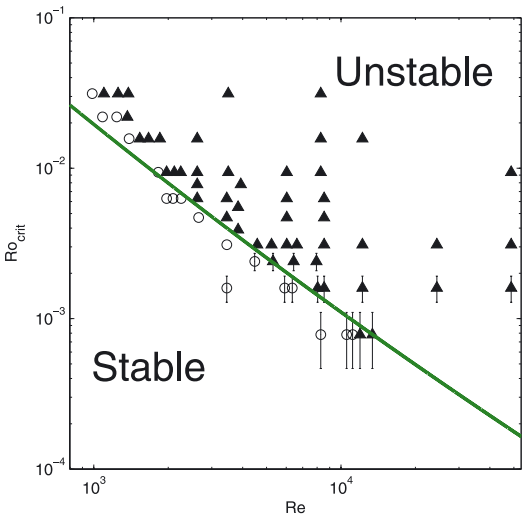

(b)

Fig. 4. (a) Dispersion relations of the Kelvin modes. The solid lines (resp. dashed lines) correspond to the first five branches of the Kelvin modes with azimuthal wavenumber $m_1 = 5$ (resp. $m_2 = 6$). Solid lines have been translated by $k = \pi/h$ and dashed lines have been translated by $\omega = 1.18$. Vertical dotted lines correspond $k = n\pi/h$, with n an integer. (b) Critical Rossby number as a function of the Reynolds number. Circles represent stable experiments and triangles unstable experiments. The theory is represented using a solid green curve. $h = 1.62$, $\omega = 1.18$.

analytically calculated (see Kudlick [15] for the peculiar case of a Kelvin mode with an azimuthal wavenumber $m = 1$ and with $\omega = 1$).

Looking for A_1 and A_2 with exponential time dependence $e^{\sigma t}$, the equation for the growth rate σ is the following

$$\left(\sigma + \frac{1}{\sqrt{Re}}S_1 + \frac{1}{Re}V_1\right)\left(\sigma + \frac{1}{\sqrt{Re}}S_2 + \frac{1}{Re}V_2\right) = |A|^2 N_1 N_2 \quad (13)$$

Table 1. Values of the parameters for the base flow (at the first resonance) and the two free Kelvin modes $m_1 = 5$ and $m_2 = 6$, $h = 1.62$.

ω	k	f	S	ξ	
1.18	1.939	− 0.452	1.86 − 0.42i	0.165	
ω_1	k_1	S_1	V_1	ξ_1	N_1
− 0.416	1.940	1.605 − 0.058i	87.159	−0.066	−0.418
ω_2	k_2	S_2	V_2	ξ_2	N_2
0.766	3.880	1.813 − 0.129i	102.676	−0.365	−0.614

The inviscid growth rate of the instability is then $\sigma = |A|\sqrt{N_1 N_2}$. The study of the signs of N_1 and N_2 (given by (10) and (11)) shows that the free Kelvin modes associated to a crossing point between branches of the dispersion relation with same monotony cannot lead to an instability. This fact was underlined using energetic methods by [16].

Including viscous effect in the calculus of σ we showed that for $h = 1.62$ and $\omega = 1.18$ (first resonance of the first Kelvin mode) the interaction between free Kelvin modes with azimuthal wavenumbers equals 5 and 6 are the most unstable, as observed in the experiments. We also plotted the stability diagram in the plane (Re,Ro) in Figure 4b. It shows (green solid curve) that the critical Rossby number scales as $Re^{-3/2}$ for $Re \ll 3000$ and as Re^{-1} for $Re \gg 3000$. These two scale factors were well confirmed by PIV measurements.

5 Weakly nonlinear theory

It is possible to add nonlinear interactions between the different modes. It results in a supplementary mode with a cylindrical symmetry and whose structure, determined experimentally, is

$$\mathbf{V_0} = A_0 J_5(d_2 r)\,\mathbf{u}_\varphi \quad (14)$$

In this expression A_0 is the amplitude of the geostrophic mode, d_2 is the second root of J_5 (i.e. $d_2 = 12.339$) and $\mathbf{u}_\varphi$ is the unit vector of the cylindrical base.

This mode is essential because it saturates the growth rate of the instability thanks to 'detuning' effects. The dynamics of the precessing flow is then entirely determined by the following amplitude equations

$$\begin{cases} \partial_t A = 2if\,Ro - \dfrac{1}{\sqrt{Re}}SA - i\xi A_0 A \\ \partial_t A_1 = A^* N_1 A_2 - \dfrac{1}{\sqrt{Re}}S_1 A_1 - i\xi_1 A_0 A_1 \\ \partial_t A_2 = A N_2 A_1 - \dfrac{1}{\sqrt{Re}}S_2 A_2 - i\xi_2 A_0 A_2 \\ \partial_t A_0 = \dfrac{1}{\sqrt{Re}}\left(\dfrac{-2}{h}A_0 + \chi_1 |A_1|^2 + \chi_2 |A_2|^2\right) \end{cases} \quad (15)$$

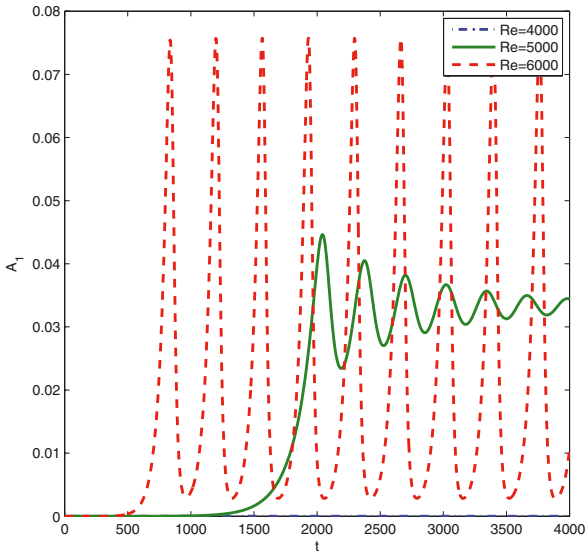

(a)

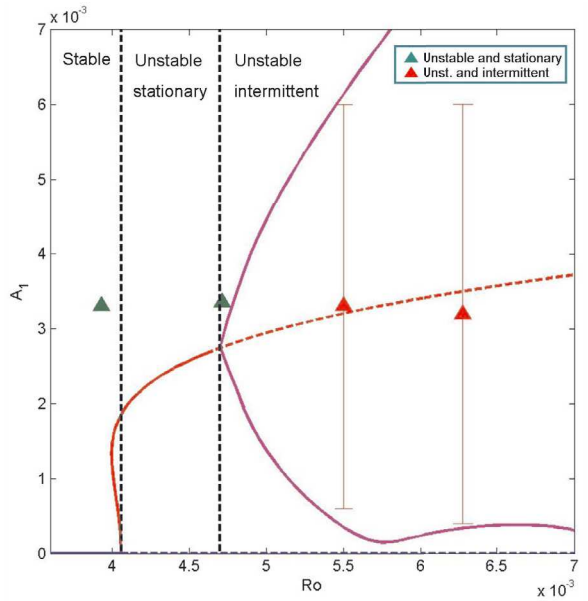

(b)

Fig. 5. (a) Amplitude of the free Kelvin mode $m_1 = 5$ as a function of the dimensionless time, for three different Reynolds numbers. For $Re = 4000$ (blue dotted line) the flow is stable. For $Re = 5000$ (green solid line) the flow is unstable and stationary. For $Re = 6000$ (red dashed line) the flow is unstable and intermittent: $h = 1.62$, $\omega = 1.18$, $Ro = 0.0031$. (b) Amplitude of the free Kelvin mode $m_1 = 5$ as a function of Ro. The bifurcation for the transition from a stable flow to an unstable flow is subcritical. The one which corresponds to the transition from an unstable and stationary flow to an unstable and intermittent flow is supercritical. The fixed point calculated from the weakly nonlinear theory is represented by the continuous red curve and is extended using a dashed line when the flow becomes unstable and intermittent. Continuous purple curves represent the maximum and the minimum of oscillations of A_1. Green triangles (resp. red) represent unstable and stationary experiments (resp. unstable and intermittent). Parameters are: $h = 1.62$, $\omega = 1.18$, $Re = 3664$.

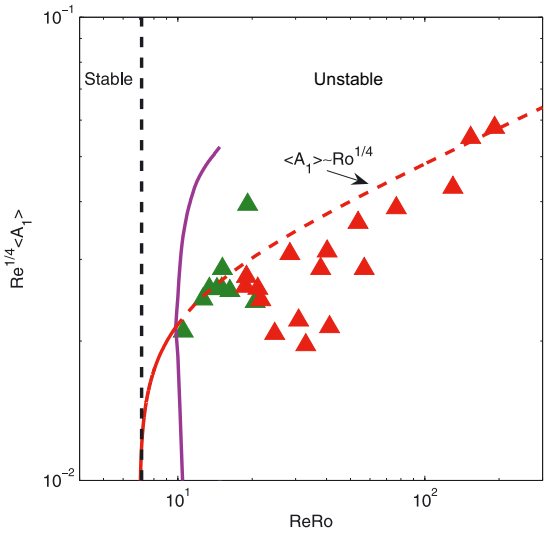

(a)

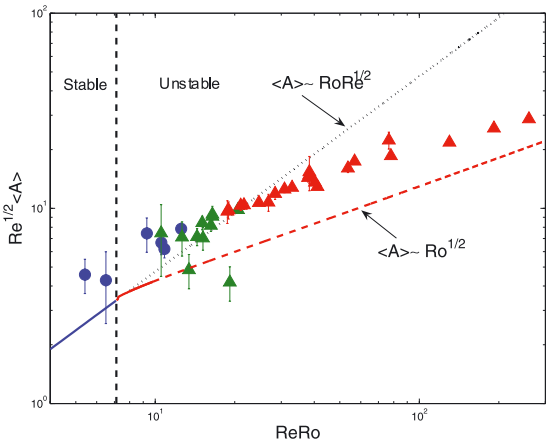

(b)

Fig. 6. Amplitude of the mode $m_1 = 5$ (a) and of the base mode (b) as a function of $RoRe$ (Volume viscous effects were neglected). The fixed point (red continuous curve and then discontinuous) is compared with the experimental mean values $\langle A_1 \rangle$ et $\langle A \rangle$. These values are represented by blue circles (stable flow), green triangles (unstable and stationary flow) or red triangles (unstable and intermittent flow). Parameters are: $h = 1.62$, $\omega = 1.18$.

Terms $\xi A_0 A$, $\xi_1 A_0 A_1$ and $\xi_2 A_0 A_2$ are the 'detuning' effects mentioned previously. They can be calculated analytically (see [11]). Terms $\chi_1 |A_1|^2$ and $\chi_2 |A_2|^2$ represent the nonlinear interactions of a free Kelvin mode with itself. They were assumed to be equal and they were fitted from experiments ($\chi_1 = \chi_2 = 10\,000$).

A numerical solution of (15) is shown in Figure 5a. Parameters are given in Table 1. Figure 5a represents the temporal evolution of A_1 as a function of the Reynolds number, for $h = 1.62$ and $\omega = 1.18$. For a Reynolds number slightly over the threshold, the instability saturates and the amplitudes (A_1 but also A, A_2 and A_0) are stationary. Amplitudes become intermittent when the

Reynolds number is increased, and the dynamics can even be chaotic for very high Reynolds numbers. This dynamics was confirmed by experiments (Fig. 5b). The resolution of (15) also showed that the instability is subcritical (Fig. 5b). Experimentally, we were not able to verify the nature of the bifurcation because it would require to vary the precessing angle with 1/100-degree increments.

For high Re, the theory showed that the fixed point of the amplitude equations only depends on $ReRo$ (Fig. 6). The amplitude A_1 (resp. A) scales as $Ro^{1/4}$ (resp. $Ro^{1/2}$) for high $ReRo$. By comparing this fixed point with the experimental mean value of the amplitudes ($\langle A\rangle$ et $\langle A_1\rangle$), we observed that the scalings are preserved and remain pertinent even if the flow becomes turbulent.

6 Conclusion

Particle Image Velocimetry measurements showed that the fluid dynamics inside a precessing cylinder consists in a stable flow for low Reynolds numbers and an unstable flow for larger Reynolds numbers. The stable flow can be predicted by a linear inviscid model and is shown to be a superposition of Kelvin modes. In the peculiar case of a resonant flow, a viscous and weakly nonlinear theory was developed to predict the amplitude saturation of the resonant Kelvin mode. This theory was confirmed by experimental results.

For larger Reynolds numbers, the structure of the unstable flow was measured using PIV. It was demonstrated that the mechanism of the precession instability is a triadic resonance between the forced base flow and two free Kelvin modes. A stability analysis based upon a this mechanism allowed to predict the most unstable free Kevin modes and to obtain an analytical expression for the growth rate. A stability diagram was also established in good agreement with experiments.

A weakly nonlinear analysis has also been carried out to take into account the interaction between the Kelvin modes. It showed that a geostrophic mode appears whose effect is to saturate the instability and that the bifurcation of the precession instability is subcritical. It also showed that, depending on the Reynolds number, the unstable flow can be steady or intermittent. Finally, the fixed point of the nonlinear amplitude equations allowed to predict correctly the scaling of the mean value mode amplitudes. Although this weakly nonlinear theory is based on a limited number of modes, it gives remarkable good results when compared to the experiments, even if the flow appears turbulent in this case.

Acknowledgements. This study was carried out under CEA-CNRS Contract No. 012171.

References

[1] W.V.R. Malkus, An experimental study of global instabilities due to tidal (elliptical) distortion of a rotating elastic cylinder, Geophys. Astrophys. Fluid Dynamics 48 (1989) 123–134
[2] A. McEwan, Inertial oscillations in a rotating fluid cylinder, J. Fluid Mech. 40 (1970) 603–640
[3] R. Manasseh, Breakdown regimes of inertia waves in a precessing cylinder, J. Fluid Mech. 243 (1992) 261–296
[4] R. Manasseh, Distortions of inertia waves in a rotating fluid cylinder forced near its fundamental mode resonance, J. Fluid Mech. 265 (1994) 345–370
[5] R. Manasseh, Nonlinear behaviour of contained inertia waves, J. Fluid Mech. 315 (1996) 151–173
[6] J. Kobine, Azimuthal flow assiociated with inertial wave resonance in a precessing cylinder, J. Fluid Mech. 319 (1996) 387–406
[7] R. Kerswell, Secondary instabilities in rapidly rotating fluids: inertial wave breakdown, J. Fluid Mech. 382 (1999) 283–306
[8] R. Kerswell, Elliptical instability, Ann. Rev. Fluid Mech. 34 (2002) 83–113
[9] C. Eloy, P. Le Gal, S. Le Dizès, Elliptic and triangular instabilities in rotating cylinders, J. Fluid Mech. 476 (2003) 357–388
[10] P. Meunier, T. Leweke, Analysis and minimization of errors due to high gradients in particle image velocimetry, Exp. Fluids 35 (2003) 408–421
[11] P. Meunier, C. Eloy, R. Lagrange, F. Nadal, A rotating fluid cylinder subject to weak precession, J. Fluid Mech. 599 (2008) 405–440
[12] H. Greenspan, The theory of rotating fluids, Cambridge University Press, 1968
[13] R. Gans, On the precession of a resonant cylinder, J. Fluid Mech. 41 (1970) 865–872
[14] R. Lagrange, Instability of a fluid inside a precessing cylinder, Physics of Fluids. 20 (2008) 081701
[15] M. Kudlick, On the transient motions in a contained rotating fluid, P.h.D. Thesis, MIT, 1966
[16] Y. Fukumoto, The three-dimensional instability of a strained vortex tube revisited, J. Fluid Mech. 493 (2003) 287318